# Electronic Supplementary Information

## X-ray absorption near-edge spectroscopy of antimony complexed with organic molecules: A theoretical interpretation

Haoze Chen[a,b], Wen Zhong[a,b], Chuanyong Jing[a,b,*]

[a] State Key Laboratory of Environmental Chemistry and Ecotoxicology, Research Center for Eco-Environmental Sciences, Chinese Academy of Sciences, Beijing 100085, China

[b] University of Chinese Academy of Sciences, Beijing 100049, China

Tel: +86 10 6284 9523; Fax: +86 10 6284 9523

*E-mail: cyjing@rcees.ac.cn

**Note S1** Species validation.

The existence of the $Sb_2(tar)_2^{2-}$ and $Sb(EDTA)^-$ species in aqueous solution was evidenced by comprehensive analysis in our previous work[1]. Fourier transform ion cyclotron resonance mass spectrometry (FT-ICR MS) analysis resolved $C_8H_4NaO_{12}Sb_2^-$ ($Sb_2tar_2Na^-$) at m/z 556.76801, 558.76849 and 560.76862. The $Sb(EDTA)^-$ was resolved at m/z 408.96378 and 410.96416 . The structures of $Sb_2(tar)_2^{2-}$ and $Sb(EDTA)^-$ in solution were also verified through XANES simulation with FPMXAN codes using DFT optimized structures.

**Note S2** Details for the TDDFT calculation.

(1) Computational details

Three types of functionals including B3LYP, B2GP-PLYP (in ωB2GP-PLYP version), and M062X were examined. The excited-state calculation was performed using the converged restricted Kohn−Sham wave functions. Scalar relativistic effects of all atoms were treated on the basis of the second order Douglas−Kroll−Hess (DKH2) methods[2]. The adapted versions of the def2 basis sets as DKH-def2-TZVP were used to describe the C, H, O, N atoms. The segmented all-electron relativistically contracted basis sets, SARC-def2-TZVP basis set was used to treat the Sb atoms to correspond to the DKH2 Hamiltonians applied. In order to accelerate the calculation, the RIJCOSX method[3] was employed. The auxiliary basis set of def2-TZVP/C and SARC/J were selected to adapt the RIJCOX method.

In TDDFT calculation, the triplet excitation and TDA approximation[4] was forbidden. The orbital window was set to enable the core electron from all Sb 1s orbitals excited to all unoccupied orbitals with other occupied orbitals fixed. In MP2 calculation from ωB2GP-PLYP cases, the “relaxed” density incorporated orbital relaxation to correct the

transition energy. The root number of excitation states for $Sb_2(tar)_2^{2-}$ complex and $Sb(EDTA)^-$ complex were 150 and 60 to calculate the region in the first 20 eV range from the transition threshold. To explore the validity of methodology to broader regions (70-80 eV at post-edge), the root number were increased to 600 and 300 at M062X/DKH-def2-TZVP level, respectively.

The orbital component of MOs and NTOs were analyzed based on modified Mulliken atom population defined by Ros & Schuit (SCPA) method and Hirshfeld method embedded in Multiwfn package. Only the half of the NTOs for $Sb_2(tar)_2^{2-}$ complex were analyzed due to the degeneracy of the transition energy. The electron-hole analysis was used to supplement the transition information in complementary with the NTO result.

(2) Data processing

Theoretical spectra were produced with the orca_mapspc utility program of the ORCA package. A constant Gaussian broadening of 0.1 and 8.0 eV was applied to the calculated transitions for Sb K-edge XAS spectra. The broadening with 0.1 eV permitted to specify the distribution of the transitions, while the broadening with 8.0 eV exactly met the FWHM of the experimental spectrum. Empirical energy shifts were applied to the calculated spectra to match the K-edge XAS spectra to align the position of the peak maximum of the white-line. The ground-state molecular orbitals (MOs) and output NTOs were visualized by VMD and VESTA software.

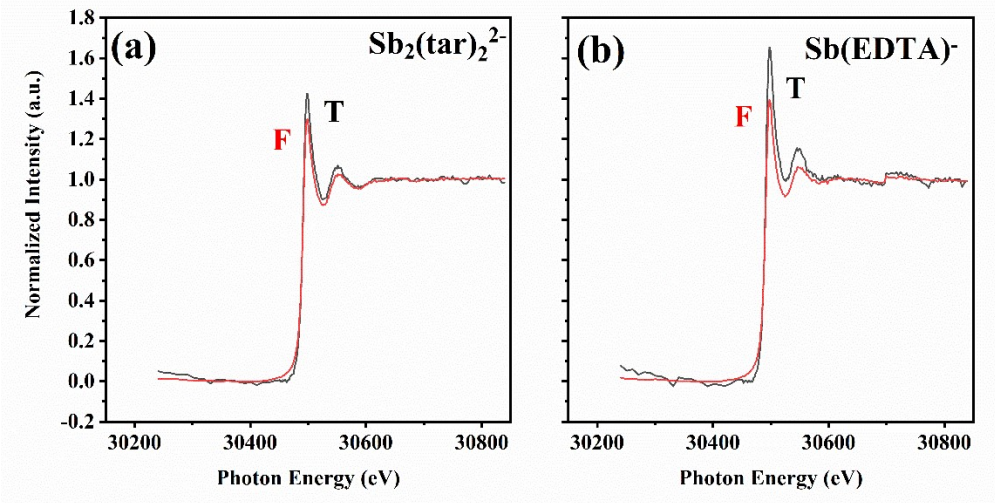


**Figure S1** The complete X-ray absorption spectrum of the solution of (a) $Sb_2(tar)_2^{2-}$ and (b) $Sb(EDTA)^-$ under transmission mode (T) and fluorescence mode (F).

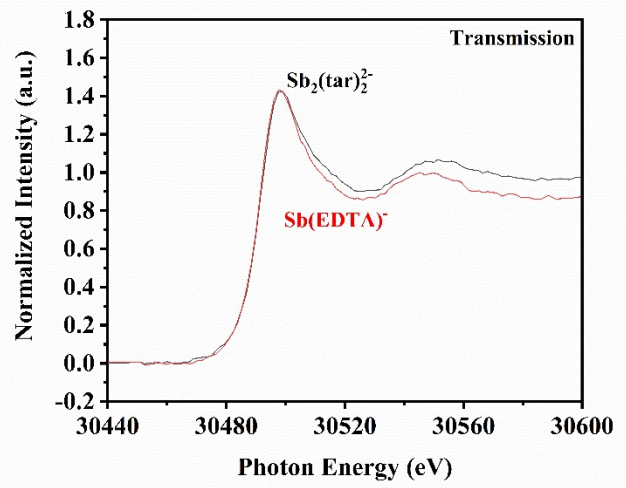


**Figure S2** The comparison of the XANES region of $Sb_2(tat)_2^{2-}$ and $Sb(EDTA)^-$ under transmission mode.

**Table S1** Transition oscillator strength for $Sb_2(tar)_2^{2-}$ complex

| State* | Excitation energy (eV)** | Transition oscillator strength (*$10^3$) | Normalized calculated intensity |
|---|---|---|---|
| S1 | 30483.311 | 39.5 | 0.83 |
| S2 | 30483.311 | 31.4 | 0.83 |
| S3 | 30483.972 | 23.1 | 0.43 |
| S4 | 30483.972 | 20.5 | 0.43 |
| S5 | 30485.873 | 51.6 | 1.00 |
| S6 | 30485.873 | 48.7 | 1.00 |
| S13 | 30491.066 | 11.4 | 0.20 |
| S14 | 30491.066 | 11.8 | 0.20 |
| S23 | 30492.797 | 9.0 | 0.22 |
| S24 | 30492.797 | 8.9 | 0.22 |

* The excited states with transition oscillator strength higher than 0.005 were listed.

** The energy indicated the unshifted excitation energy.

**Table S2** Transition oscillator strength for $Sb(EDTA)^-$ complex

| States | Excitation energy (eV)* | Transition oscillator strength (*$10^3$) | Normalized calculated intensity |
|---|---|---|---|
| S1 | 30483.450 | 0.7 | 0.02 |
| S2 | 30484.117 | 14.4 | 0.94 |
| S3 | 30484.509 | 14.6 | 1.00 |
| S17 | 30493.003 | 1.0 | 0.07 |
| S18 | 30493.401 | 1.0 | 0.07 |

* The excited states with transition oscillator strength higher than 0.001 were listed except for S1.

** The energy indicated the unshifted excitation energy.

**Note S3** Transition components (contribution from the molecular orbital pairs) of the theoretical XANES calculation for $Sb_2(tar)_2^{2-}$ complex. The weights of the individual excitations are omitted if less than 0.05. The unoccupied molecular orbitals highlighted (> 0.20) were plotted in **Figure S3**. The contribution of the atomic groups to MOs were listed in **Table S3** and **Table S4**.

STATE 1: E= 30483.311 eV

**1a → 126a : 0.404701 1a → 127a : 0.374568**

STATE 2: E= 30483.311 eV

**0a → 126a : 0.404647 0a → 127a : 0.374619**

STATE 3: E= 30483.972 eV

0a → 126a : 0.071698 0a → 127a : 0.062177

**0a → 128a : 0.361765 0a → 129a : 0.343597**

STATE 4: E= 30483.972 eV

1a → 126a : 0.071681 1a → 127a : 0.062192

**1a → 128a : 0.361711 1a → 129a : 0.343645**

STATE 5: E= 30485.873 eV

**1a → 130a : 0.273558** 1a → 131a : 0.129692

1a → 134a : 0.090587 1a → 135a : 0.095585

1a → 139a : 0.063040

STATE 6: E= 30485.873 eV

**0a → 130a : 0.273571** 0a → 131a : 0.129640

0a → 134a : 0.090669 0a → 135a : 0.095523

0a → 139a : 0.063055

STATE 13: E= 30491.066 eV

**0a → 131a : 0.213207** 0a → 132a : 0.107239

0a → 138a : 0.110718 0a → 139a : 0.069166

STATE 14: E= 30491.066 eV

**1a → 131a : 0.213178** 1a → 132a : 0.107320

1a → 138a : 0.110770 1a → 139a : 0.069163

STATE 23: E= 30492.797 eV

1a → 134a : 0.138422 1a → 135a : 0.151129

1a → 149a : 0.095934 1a → 150a : 0.065856

1a → 156a : 0.103938 1a → 157a : 0.052389

STATE 24: E= 30492.797 eV

0a → 134a : 0.138400 0a → 135a : 0.151124

0a → 149a : 0.095642 0a → 150a : 0.066224

0a → 156a : 0.104051 0a → 157a : 0.052382

**Note S4** Transition components (contribution from the molecular orbital pairs) of the theoretical XANES calculation for $Sb(EDTA)^-$ complex. The weights of the individual excitations are omitted if less than 0.05. The unoccupied molecular orbitals highlighted (> 0.20) were plotted in **Figure S4** and **Figure S5** from different perspective. The contribution of the atomic groups to MOs were listed in **Table S5** and **Table S6**.

STATE 1: E= 30483.450 eV

**0a → 101a : 0.538860 0a → 102a : 0.358450**

STATE 2: E= 30484.117 eV

**0a → 103a : 0.564567** 0a → 105a : 0.106125

0a → 107a : 0.071666 0a → 109a : 0.138521

STATE 3: E= 30484.509 eV

0a → 103a : 0.137737 0a → 104a : 0.051010

0a → 105a : 0.102413 **0a → 107a : 0.505774**

STATE 17: E= 30493.003 eV

0a → 110a : 0.056236 0a → 113a : 0.140613

**0a → 115a : 0.215337** 0a → 119a : 0.131939

0a → 120a : 0.094015 0a → 135a : 0.051375

STATE 18: E= 30493.401 eV

0a → 113a : 0.055548 **0a → 115a : 0.416822**

0a → 117a : 0.090901 0a → 129a : 0.050291

0a → 140a : 0.052805

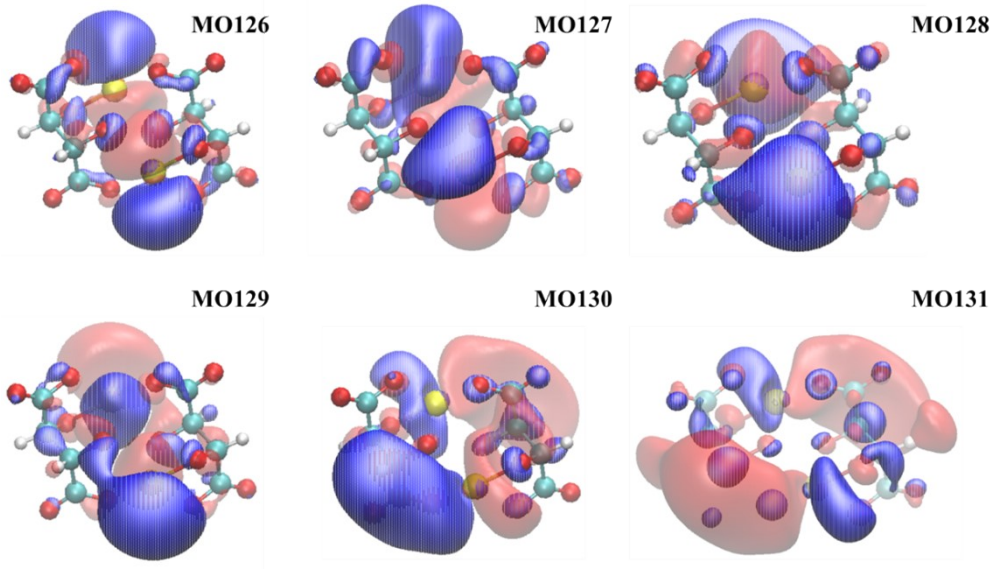


**Figure S3** Frontier unoccupied molecular orbital for $Sb_2(tar)_2^{2-}$ complex (top view).

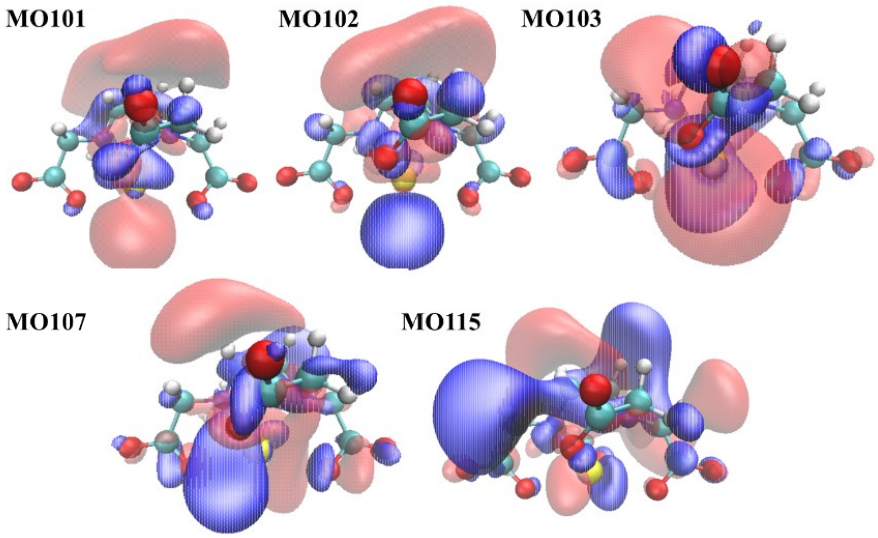


**Figure S4** Frontier unoccupied molecular orbital for Sb(EDTA)$^-$ complex (front view).

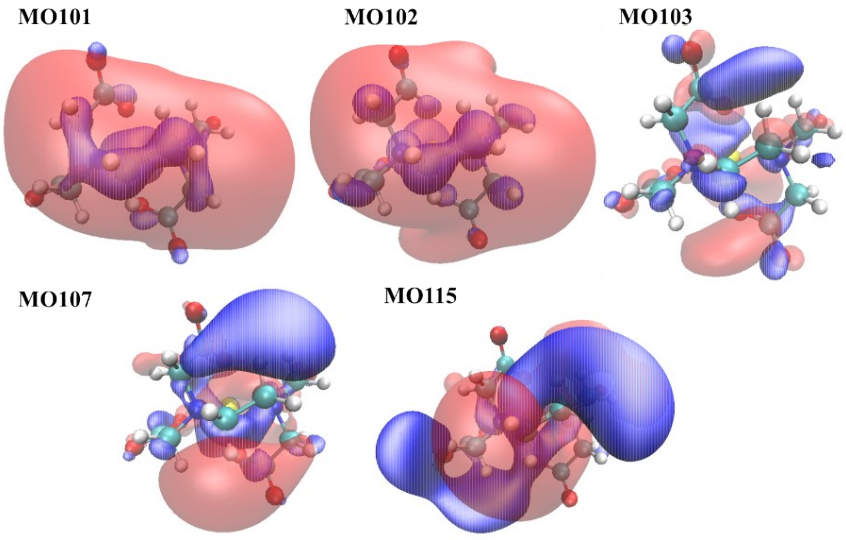


**Figure S5** Frontier unoccupied molecular orbital for Sb(EDTA)$^-$ complex (top view).

**Note S5** Description for the frontier molecular orbital shown in **Figure S3**.

MO126 is the LUMO of $Sb_2(tar)_2^{2-}$ complex which consisted of major antiparallel *p* orbitals. Minor contribution was from nearby deprotonated hydroxyl group and carbon chain. MO127 possessed energy level close to MO126, but the *p* orbitals are parallel in

another direction. The *p* orbitals in MO126 and MO127 are vertical to Sb-O bonds. MO126 and MO127 majorly contributes to the S1 states. However, in MO128 and MO129, antimony centers connect to nearby coordinated oxygens with $sp^3$ hybrid orbitals. The nodes between antimony and oxygen can be observed. The characteristic can be summarized as σ* orbitals. Based on the bimetallic nature, two similar σ* orbitals can be observed in one molecule. In MO128, the two orbitals are antiparallel, while in MO129, they are parallel in another direction. In the cases of MO130 and MO131, the *p* orbitals contributed less to the molecular orbitals. The *p* orbitals formed nodes with all coordinated oxygen atoms. This feature can be summarized as another type of σ*. All mentioned orbitals were responsible for the transitions in the major peaks of the white-line.

**Note S6** Description for the frontier molecular orbital shown in **Figure S4 and S5**.

The contribution of antimony to the molecular orbital in $Sb(EDTA)^-$ complex was smaller than that in $Sb_2(tar)_2^{2-}$ complex. In most cases, the major contribution to the molecular orbital was attributed to the carbon chains between two tertiary nitrogen atoms, critically, to only the carbon atoms. Although contribution of antimony is small, the *p* orbitals for antimony still can be visualized in **Figure S4**. MO101 is the LUMO of $Sb(EDTA)^-$ complex. In MO101 and MO102, the 2s orbitals in noncarboxylic carbon atoms formed bonding orbitals. Then the group orbital interacts with the vertical *p* orbital from antimony. In other cases, it's hard to specify the nature of molecular orbitals.

**Table S3** Composition of the molecular orbital for $Sb_2(tar)_2^{2-}$ complex shown in **Figure S3** (SCPA)

| | E (eV)* | Sb | | Coordinated atom | | | $C_\alpha H$** | | $C_\beta OO$ | Major component |
|---|---|---|---|---|---|---|---|---|---|---|
| | | Sb% | Sb p% | $O_\alpha$% | $O_\beta$% | $O_\beta$ s% | tot% | s % | tot% | |
| MO-0 | -30486.17 | 100.0 | 0.0 | | | | | | | Sb 1s |
| MO-126 | 7.34 | 45.8 | 38.4 | 13.1 | 3.1 | 1.4 | 35.2 | 23.0 | 6.0 | Sb 5p + $O_\alpha C_\alpha H$ (s) |
| MO-127 | 7.48 | 49.5 | 46.5 | 5.2 | 13.2 | 6.9 | 22.4 | 19.7 | 22.9 | Sb 5p + $C_\alpha H$ (s)+ $C_\beta OO$ |
| MO-128 | 8.05 | 50.7 | 33.8 | 6.0 | 6.8 | | 31.0 | 15.0 | 12.3 | Sb + $C_\alpha H$ |
| MO-129 | 8.23 | 53.9 | 31.0 | 7.2 | 2.3 | | 35.0 | 30.4 | 4.0 | Sb + $C_\alpha H$ (s) |
| MO-130 | 8.78 | 15.7 | 14.0 | 6.7 | 3.8 | 3.3 | 61.0 | 52.0 | 16.7 | $C_\alpha H$ (s) |
| MO-131 | 9.15 | 7.7 | 6.7 | 0.7 | 1.2 | | 84.5 | 70.1 | 7.1 | $C_\alpha H$ (s) |

* The energy indicated the eigenvalues of the Kohn-Sham equation.

** The species $C_\alpha H$ indicated the hydrocarbon chains.

The species $C_\beta$ indicated the carbon atoms of carboxyl group, while $O_\beta$ indicated the coordinated oxygen.

The species $O_\alpha$ indicated oxygen of noncarboxylic hydroxyl group.

**Table S4** Composition of the molecular orbital for $Sb_2(tar)_2^{2-}$ complex shown in **Figure S3** (Hirshfeld)

| | E (eV)* | Sb | | Coordinated atom | | $C_\alpha H$ | $C_\beta OO$ | Major component |
|---|---|---|---|---|---|---|---|---|
| | | Sb1% | Sb2% | $O_\alpha$% | $O_\beta$% | tot% | tot% | |
| MO-0 | -30486.17 | 100.0 | | | | | | Sb 1s |
| MO-1 | -30486.17 | | 100% | | | | | Sb 1s |
| MO-126 | 7.34 | 35.2 | 35.2 | 15.2 | 6.6 | 4.5 | 9.9 | Sb |
| MO-127 | 7.48 | 33.2 | 33.2 | 8.5 | 14.3 | 4.9 | 20.2 | Sb + $COO_\beta$ |
| MO-128 | 8.05 | 33.2 | 33.2 | 9.2 | 12.7 | 6.3 | 18.1 | Sb |
| MO-129 | 8.23 | 33.0 | 33.0 | 18.2 | 6.3 | 6.1 | 9.7 | Sb |
| MO-130 | 8.78 | 18.8 | 18.8 | 12.0 | 6.5 | 29.0 | 21.4 | Sb + $C_\alpha H$ |
| MO-131 | 9.15 | 14.2 | 14.2 | 5.5 | 5.0 | 46.6 | 19.5 | Sb + $C_\alpha H$ |

* The energy indicated the eigenvalues of the Kohn-Sham equation.

**Table S5** Composition of the molecular orbital for $Sb(EDTA)^-$ complex shown in **Figure S4 (**SCPA**)**

| | E (eV)* | Sb | | Coordinated atom | | $C_\alpha H$ ** | | $C_\beta H$%** | | $C_\gamma OO$%** | Component |
|---|---|---|---|---|---|---|---|---|---|---|---|
| | | Sb% | Sb p% | $O_\alpha$% | N% | tot% | s% | tot% | s% | tot% | |
| MO-0 | -30489.51 | 100.0 | 0.0 | | | | | | | | Sb 1s |
| MO-101 | 4.16 | 5.7 | 3.9 | 0.7 | 10.0 (s) | 66.2 | 58.7 | 15.9 | 14.3 | 2.2 | $C_\alpha H$ (s) |
| MO-102 | 4.82 | 6.9 | 3.3 | 0.3 | 2.8 (p) | 73.4 | 67.0 | 13.0 | 8.6 | 3.9 | $C_\alpha H$ (s) |
| MO-103 | 5.00 | 9.9 | 9.5 | 3.3 | 3.7 (p) | 53.9 | 45.3 | 24.6 | 22.4(p) | 7.9 | $C_\alpha H$ (s) + $C_\beta H$ (p) |
| MO-107 | 5.91 | 2.7 | 2.1 | 1.2 | 9.4 (s) | 69.3 | 61.9 | 15.6 | 14.0 | 3.1 | $C_\alpha H$ (s) |
| MO-115 | 7.36 | 0.1 | | 0.2 | 1.8 (p) | 74.7 | 70.1 | 21.7 | 19.7 | 1.6 | $C_\alpha H$ (s) + $C_\beta H$ (s) |

* The energy indicated the eigenvalues of the Kohn-Sham equation.

** The species $C_\alpha H$ indicated the hydrocarbon chain between two nitrogen atoms.

The species $C_\beta H$ indicated the hydrocarbon chains between nitrogen atoms and carboxyl groups, while $O_\alpha$ and $O_\beta$ indicated the coordinated oxygen and the non-coordinated oxygen.

**Table S6** Composition of the molecular orbital for $Sb(EDTA)^-$ complex shown in **Figure S4 (**Hirshfeld**)**

| | E (eV)* | Sb | Coordinated atom | | $C_\alpha H$ | $C_\beta H$% | $C_\gamma OO$% | Component |
|---|---|---|---|---|---|---|---|---|
| | | Sb% | $O_\alpha$% | N% | tot% | tot% | tot% | |
| MO-0 | -30489.51 | 100.0 | | | | | | Sb 1s |
| MO-101 | 4.16 | 35.0 | 6.2 | 6.7 | 30.5 | 18.1 | 9.7 | Sb + $C_\alpha H$ |
| MO-102 | 4.82 | 27.0 | 5.8 | 9.6 | 33.5 | 18.6 | 11.3 | Sb + $C_\alpha H$ |
| MO-103 | 5.00 | 47.2 | 18.0 | 2.2 | 8.5 | 9.3 | 32.8 | Sb + $C_\gamma OO$ |
| MO-107 | 5.91 | 38.4 | 16.7 | 4.1 | 18.7 | 13.9 | 24.9 | Sb + $C_\gamma OO$ |
| MO-115 | 7.36 | 4.2 | 4.3 | 4.4 | 39.1 | 36.3 | 16.1 | $C_\alpha H$ + $C_\beta H$ |

* The energy indicated the eigenvalues of the Kohn-Sham equation.

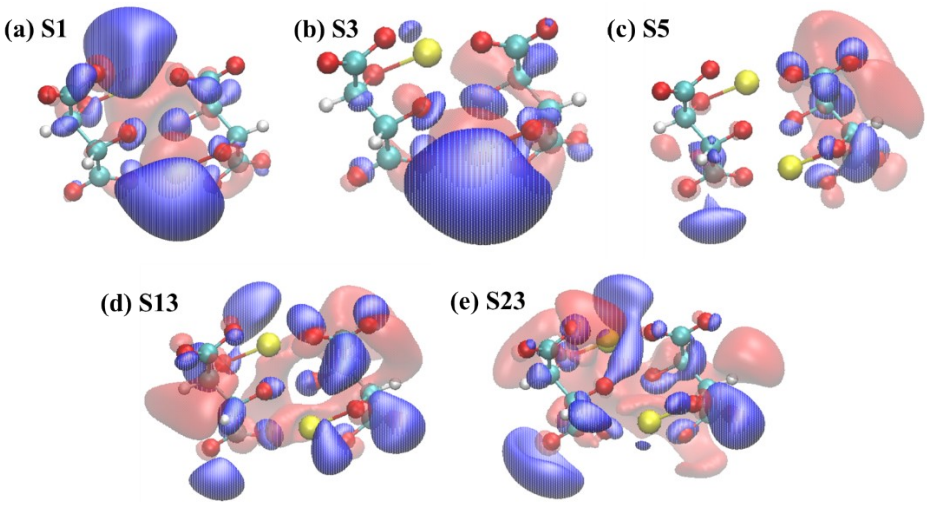


212

213 **Figure S6** Electron NTOs for $Sb_2(tar)_2^{2-}$ complex.

214

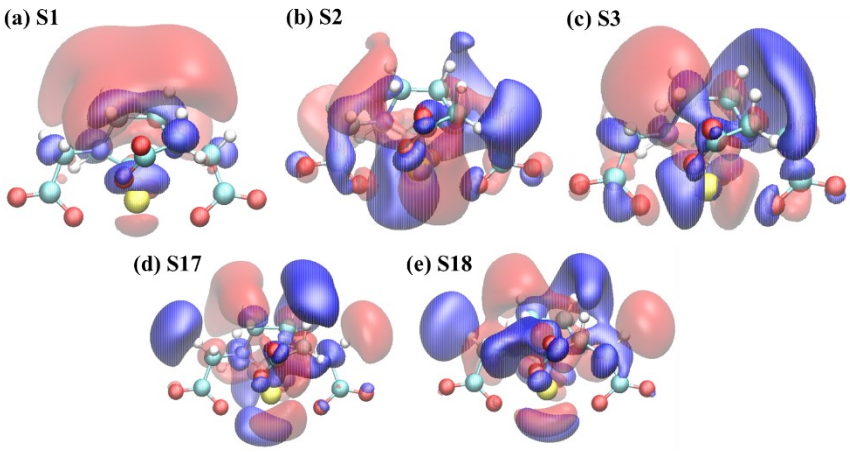


215

216 **Figure S7** Electron NTOs for $Sb(EDTA)^-$ complex.

217

218

219

220

221

222

223

224

**Table S7** Composition of the electron NTO for $Sb_2(tar)_2^{2-}$ complex (SCPA)

| | $E_{trans}$ (eV) * | Sb | | Coordinated atom | | Functional group | | Major component |
|---|---|---|---|---|---|---|---|---|
| | | Sb% | Sb 5p% | $C_\alpha H$ % | $C_\beta OO$ % | $C_\alpha H$ % | $C_\beta OO$ % | |
| S1/S2 | 30495.81 | 38.0 | 26.9 | 34.1 | 19.2 | 34.1 | 19.2 | Sb 5p + $C_\alpha H$ |
| S3/S4 | 30496.47 | 23.5 | 15.5 | 58.2 | 13.0 | 58.2 | 13.0 | Sb 5p + $C_\alpha H$ |
| S5/S6 | 30498.37 | 3.1 | 1.5 | 69.4 | 24.9 | 69.4 | 24.9 | $C_\alpha H$ + $C_\beta OO$ |
| S13/S14 | 30503.57 | 4.6 | 1.5 | 66.9 | 26.6 | 66.9 | 26.6 | $C_\alpha H$ + $C_\beta OO$ |
| S23/S24 | 30505.3 | 6.6 | 2.7 | 45.0 | 41.2 | 45.0 | 41.2 | $C_\alpha H$ + $C_\beta OO$ |

* The transition energy was calculated from the sum of calculated value and the energy shift of 12.5 eV.

**Table S8** Composition of the electron NTO for $Sb_2(tar)_2^{2-}$ complex (Hirshfeld)

| | $E_{trans}$ (eV) * | Sb | | Coordinated atom | | Functional group | | Major component |
|---|---|---|---|---|---|---|---|---|
| | | Sb1% | Sb2% | $O_\alpha$% | $O_\beta$% | $C_\alpha H$ % | $C_\beta OO$ % | |
| S1/2 | 30495.81 | 42.4 | 24.4 | 11.8 | 9.2 | 6.6 | 14.8 | Sb |
| S3/4 | 30496.47 | 2.5 | 61.1 | 13.6 | 11.0 | 6.4 | 16.4 | |
| S5/6 | 30498.37 | 4.1 | 3.6 | 3.5 | 6.4 | 46.3 | 42.5 | |
| S13/14 | 30503.57 | 9.5 | 6.8 | 6.9 | 10.9 | 29.2 | 47.7 | $C_\alpha H$ + $C_\beta OO$ |
| S23/24 | 30505.30 | 15.1 | 6.3 | 11.4 | 12.8 | 28.0 | 39.2 | |

* The transition energy was calculated from the sum of calculated value and the energy shift of 12.5 eV.

**Table S9** Composition of the electron NTO for $Sb(EDTA)^-$ complex (SCPA)

| | $E_{trans}$ (eV) * | Sb | | Coordinated atom | | Functional group | | | Major component |
|---|---|---|---|---|---|---|---|---|---|
| | | Sb% | Sb 5p% | $O_\alpha$% | N% | $C_\alpha H$% | $C_\beta H$% | $C_\gamma OO$% | |
| S1 | 30494.45 | 3.2 | 0.6 | 0.0 | 2.3 | 75.6 | 16.9 | 2.0 | |
| S2 | 30495.12 | 3.3 | 2.8 | 1.0 | 4.7 | 56.9 | 28.6 | 6.7 | $C_\alpha H$ |
| S3 | 30495.51 | 0.6 | < 0.6 | 0.4 | 6.7 | 73.5 | 14.8 | 4.3 | $C_\alpha H + C_\beta H$ |
| S17 | 30504.00 | 1.3 | 1.2 | 0.6 | 1.1 | 51.3 | 37.9 | 8.5 | $C_\beta H$ |
| S18 | 30504.40 | 1.5 | 1.4 | 0.4 | 4.4 | 72.2 | 20.0 | 2.0 | $C_\alpha H + C_\beta H$ |

* The transition energy was calculated from the sum of calculated value and the energy shift of 11.0 eV.

**Table S10** Composition of the electron NTO for $Sb(EDTA)^-$ complex for the local structure (Hirshfeld)

| | $E_{trans}$ (eV) * | Sb | Coordinated atom | | Functional group | | | Major component |
|---|---|---|---|---|---|---|---|---|
| | | Sb% | $O_\alpha$% | N% | $C_\alpha H$% | $C_\beta H$% | $C_\gamma OO$% | |
| S1 | 30494.45 | 4.4 | 1.4 | 1.3 | 59.2 | 29.2 | 5.9 | $C_\alpha H + C_\beta H$ |
| S2 | 30495.12 | 30.2 | 15.6 | 2.7 | 10.7 | 24.2 | 32.2 | Sb 5p + $C_\beta H$ + $C_\gamma OO$ |
| S3 | 30495.51 | 16.5 | 8.8 | 2.9 | 34.6 | 26.8 | 19.1 | $C_\alpha H + C_\beta H$ |
| S17 | 30504.00 | 7.7 | 5.0 | 2.5 | 29.8 | 42.5 | 17.5 | |
| S18 | 30504.40 | 6.8 | 8.9 | 3.0 | 29.6 | 36.0 | 24.6 | $C_\alpha H + C_\beta H + C_\gamma OO$ |

* The transition energy was calculated from the sum of calculated value and the energy shift of 11.0 eV.

**Table S11** Atomic composition of the electron NTO for $Sb_2(tar)_2^{2-}$ complex (SCPA)

| Species* | | S1 | S3 | S5 | S13 | S23 |
|---|---|---|---|---|---|---|
| $C_\alpha H$ | C1 | 14.5% | 20.3% | 32.4% | 24.4% | 5.1% |
| | C2 | 2.3% | 23.9% | 1.0% | 6.9% | 4.6% |
| | C11 | 1.2% | 8.8% | 0.7% | 7.5% | 6.6% |
| | C12 | 11.9% | 3.5% | 9.7% | 20.1% | 22.5% |
| | H23 | 1.6% | 0.3% | 22.8% | 6.1% | 1.0% |
| | H9 | 0.1% | 0.0% | 2.1% | 0.2% | 2.6% |
| | H20 | 0.2% | 0.9% | 0.4% | 1.3% | 0.6% |
| | H24 | 2.2% | 0.5% | 0.3% | 0.4% | 2.2% |
| $C_\beta$ | C3 | 1.6% | 1.3% | 5.2% | 2.2% | 0.2% |
| | C4 | 1.7% | 4.1% | 2.3% | 1.3% | 3.9% |
| | C13 | 4.9% | 2.3% | 0.7% | 6.4% | 2.2% |
| | C14 | 2.5% | 1.0% | 5.7% | 7.2% | 17.4% |
| $O_\alpha$ | O10 | 0.3% | 0.2% | 0.7% | 0.3% | 1.3% |
| | O19 | 0.9% | 0.0% | 0.3% | 0.6% | 2.3% |
| | O21 | 0.8% | 0.9% | 1.2% | 0.8% | 1.8% |
| | O22 | 6.7% | 4.3% | 0.4% | 0.4% | 1.8% |
| $O_\beta$ | O5 | 0.4% | 0.1% | 0.2% | 0.2% | 0.2% |
| | O7 | 3.4% | 0.6% | 1.3% | 0.9% | 3.2% |
| | O16 | 1.4% | 2.1% | 0.3% | 2.2% | 2.3% |
| | O18 | 1.1% | 0.1% | 0.2% | 0.2% | 3.3% |
| $O_\gamma$ | O6 | 0.0% | 0.7% | 1.1% | 0.1% | 0.4% |
| | O8 | 0.3% | 0.4% | 3.8% | 1.6% | 0.1% |
| | O15 | 1.8% | 0.1% | 0.0% | 0.1% | 0.5% |
| | O17 | 0.2% | 0.3% | 4.3% | 4.3% | 7.6% |
| Sb | Sb25 | 15.7% | 0.9% | 1.8% | 4.0% | 5.9% |
| | Sb26 | 22.3% | 22.6% | 1.3% | 0.6% | 0.7% |

**Table S12** Atomic composition of the electron NTO for $Sb_2(tar)_2^{2-}$ complex (Hirshfeld)

242

| Species* | | S1 | S3 | S5 | S13 | S23 |
|---|---|---|---|---|---|---|
| $C_\alpha H$ | C1 | 1.7 | 2.2 | 9.6 | 5.5 | 3.5 |
| | C2 | 0.4 | 0.8 | 3.9 | 3.9 | 6.2 |
| | C11 | 1.0 | 0.4 | 0.8 | 2.3 | 1.9 |
| | C12 | 0.8 | 0.8 | 1.1 | 1.9 | 1.4 |
| | H23 | 1.1 | 1.0 | 24.6 | 7.3 | 2.7 |
| | H9 | 0.3 | 0.1 | 4.6 | 2.8 | 8.5 |
| | H20 | 0.4 | 0.4 | 0.8 | 2.5 | 1.9 |
| | H24 | 0.9 | 0.7 | 1.0 | 2.9 | 1.8 |
| $C_\beta$ | C3 | 1.3 | 0.5 | 8.2 | 14.1 | 0.8 |
| | C4 | 0.8 | 1.2 | 7.5 | 2.5 | 7.0 |
| | C13 | 0.9 | 0.2 | 0.3 | 1.9 | 1.8 |
| | C14 | 0.8 | 1.6 | 3.5 | 2.7 | 3.5 |
| $O_\alpha$ | O10 | 1.6 | 2.8 | 1.2 | 1.8 | 2.5 |
| | O19 | 2.4 | 0.3 | 0.8 | 2.0 | 4.1 |
| | O21 | 1.8 | 2.5 | 0.4 | 0.9 | 1.1 |
| | O22 | 6.1 | 8.0 | 1.1 | 2.1 | 3.7 |
| $O_\beta$ | O5 | 1.3 | 0.2 | 2.3 | 5.5 | 1.0 |
| | O7 | 1.7 | 3.9 | 2.6 | 1.8 | 4.6 |
| | O16 | 2.4 | 6.7 | 1.2 | 2.9 | 3.3 |
| | O18 | 3.7 | 0.1 | 0.2 | 0.7 | 3.8 |
| $O_\gamma$ | O6 | 0.3 | 0.8 | 5.2 | 1.2 | 3.8 |
| | O8 | 0.4 | 0.2 | 7.1 | 9.1 | 1.3 |
| | O15 | 0.8 | 0.1 | 0.2 | 1.7 | 1.0 |
| | O17 | 0.3 | 0.8 | 4.1 | 3.5 | 7.2 |
| Sb | Sb25 | 42.4 | 2.5 | 4.1 | 9.5 | 15.1 |
| | Sb26 | 24.4 | 61.1 | 3.6 | 6.8 | 6.3 |

243

244

245

246 **Table S13** Atomic composition of the electron NTO for $Sb(EDTA)^-$ complex (SCPA)

| Species | | S1 | S2 | S3 | S17 | S18 |
|---|---|---|---|---|---|---|
| $C_\alpha H$ | C1 | 26.0% | 25.8% | 34.1% | 21.5% | 12.4% |
| | H2 | 10.2% | 1.0% | 0.3% | 2.0% | 0.3% |
| | H3 | 1.6% | 1.7% | 2.4% | 2.2% | 0.5% |
| | C4 | 26.0% | 25.8% | 34.1% | 21.5% | 12.4% |
| | H5 | 1.6% | 1.7% | 2.4% | 2.2% | 0.5% |
| | H6 | 10.2% | 1.0% | 0.3% | 2.0% | 0.3% |
| N | N7 | 1.1% | 2.3% | 3.3% | 0.6% | 1.0% |
| | N8 | 1.1% | 2.3% | 3.3% | 0.6% | 1.0% |
| $C_\beta H$ | C9 | 2.1% | 9.6% | 5.3% | 13.4% | 17.2% |
| | H10 | 0.5% | 1.3% | 0.1% | 2.6% | 0.0% |
| | H11 | 0.3% | 2.3% | 0.4% | 0.3% | 0.3% |
| | C12 | 3.2% | 0.9% | 1.2% | 1.3% | 2.5% |
| | H13 | 0.9% | 0.2% | 0.2% | 0.0% | 0.2% |
| | H14 | 1.5% | 0.1% | 0.2% | 1.3% | 0.2% |
| | C15 | 2.1% | 9.6% | 5.3% | 13.4% | 17.2% |
| | H16 | 0.5% | 1.3% | 0.1% | 2.6% | 0.0% |
| | H17 | 0.3% | 2.3% | 0.4% | 0.3% | 0.3% |
| | C18 | 3.2% | 0.9% | 1.2% | 1.3% | 2.5% |
| | H19 | 0.9% | 0.2% | 0.2% | 0.0% | 0.2% |
| | H20 | 1.5% | 0.1% | 0.2% | 1.3% | 0.2% |
| $C_\gamma$ | C21 | 0.6% | 0.9% | 1.4% | 2.5% | 6.6% |
| | C22 | 0.6% | 0.9% | 1.4% | 2.5% | 6.6% |
| | C23 | 0.4% | 0.4% | 0.5% | 1.1% | 2.3% |
| | C24 | 0.4% | 0.4% | 0.5% | 1.1% | 2.3% |
| $O_\alpha$ | O25 | 0.0% | 1.3% | 0.0% | 0.2% | 0.4% |
| | O27 | 0.0% | 1.3% | 0.0% | 0.2% | 0.4% |
| | O28 | 0.0% | 0.3% | 0.0% | 0.1% | 0.3% |
| | O30 | 0.0% | 0.3% | 0.0% | 0.1% | 0.3% |
| $O_\beta$ | O26 | 0.0% | 0.3% | 0.1% | 0.3% | 1.0% |
| | O29 | 0.0% | 0.2% | 0.1% | 0.0% | 3.2% |
| | O31 | 0.0% | 0.3% | 0.1% | 0.3% | 1.0% |
| | O32 | 0.0% | 0.2% | 0.1% | 0.0% | 3.2% |
| Sb | Sb33 | 3.2% | 3.3% | 0.6% | 1.3% | 3.4% |

**Table S14** Atomic composition (%) of the electron NTO for $Sb(EDTA)^-$ complex (Hirshfeld)

| Species | | S1 | S2 | S3 | S17 | S18 |
|---|---|---|---|---|---|---|
| $C_\alpha H$ | C1 | 8.1 | 1.4 | 5.1 | 3.5 | 4.8 |
| | H2 | 16.8 | 1.9 | 4.2 | 7.7 | 5.7 |
| | H3 | 4.7 | 2.0 | 8.0 | 3.7 | 4.3 |
| | C4 | 8.1 | 1.4 | 5.1 | 3.5 | 4.8 |
| | H5 | 4.7 | 2.0 | 8.0 | 3.7 | 4.3 |
| | H6 | 16.8 | 1.9 | 4.2 | 7.7 | 5.7 |
| N | N7 | 0.7 | 1.4 | 1.4 | 1.2 | 1.5 |
| | N8 | 0.7 | 1.4 | 1.4 | 1.2 | 1.5 |
| $C_\beta H$ | C9 | 1.3 | 2.3 | 2.5 | 2.6 | 3.6 |
| | H10 | 1.7 | 2.3 | 1.9 | 7.2 | 8.0 |
| | H11 | 1.4 | 3.0 | 4.0 | 1.2 | 2.0 |
| | C12 | 2.6 | 1.9 | 1.6 | 3.1 | 1.6 |
| | H13 | 1.5 | 1.9 | 1.6 | 1.1 | 1.2 |
| | H14 | 6.1 | 0.8 | 1.9 | 6.0 | 1.6 |
| | C15 | 1.3 | 2.3 | 2.6 | 2.6 | 1.2 |
| | H16 | 1.7 | 2.3 | 1.9 | 7.2 | 8.0 |
| | H17 | 1.4 | 3.0 | 4.0 | 1.2 | 2.0 |
| | C18 | 2.6 | 1.9 | 1.6 | 3.1 | 1.6 |
| | H19 | 1.5 | 1.9 | 1.6 | 1.1 | 1.2 |
| | H20 | 6.1 | 0.8 | 1.9 | 6.0 | 1.6 |
| $C_\gamma$ | C21 | 0.4 | 2.5 | 1.3 | 0.9 | 1.0 |
| | C22 | 0.4 | 2.5 | 1.3 | 0.9 | 1.0 |
| | C23 | 1.2 | 3.0 | 2.2 | 2.8 | 4.1 |
| | C24 | 1.2 | 3.0 | 2.2 | 2.8 | 4.1 |
| $O_\alpha$ | O25 | 0.2 | 3.4 | 2.6 | 0.8 | 0.7 |
| | O27 | 0.2 | 3.4 | 2.6 | 0.8 | 0.7 |
| | O28 | 0.5 | 4.4 | 1.8 | 1.7 | 3.8 |
| | O30 | 0.5 | 4.4 | 1.8 | 1.7 | 3.8 |
| $O_\beta$ | O26 | 0.5 | 1.1 | 1.0 | 1.8 | 2.2 |
| | O29 | 0.1 | 1.6 | 0.7 | 0.7 | 0.6 |
| | O31 | 0.5 | 1.1 | 1.0 | 1.8 | 2.2 |
| | O32 | 0.1 | 1.6 | 0.7 | 0.7 | 0.6 |
| Sb | Sb33 | 4.4 | 30.1 | 16.5 | 7.7 | 6.8 |

250

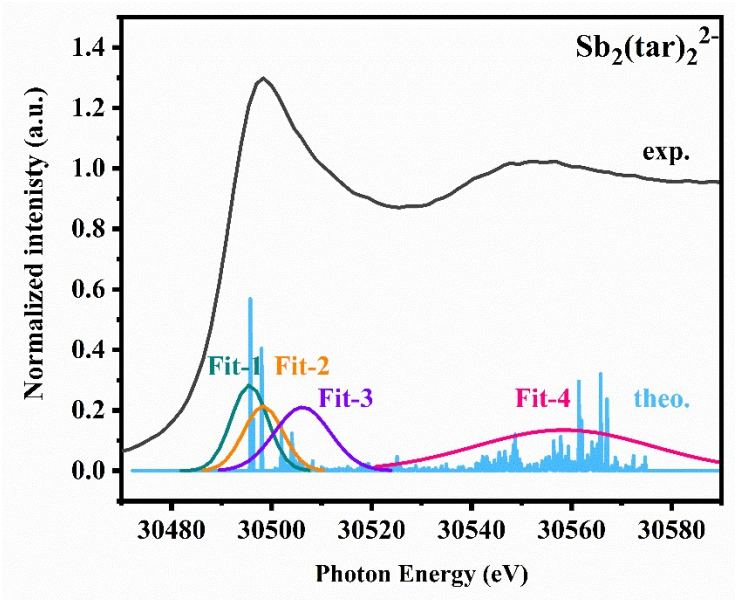


251

252 **Figure S8** Experimental and simulated Sb K-edge X-ray absorption spectrum of
253 $Sb_2(tar)_2^{2-}$ complex. The subpeaks of experimental spectrum were result from peak
254 fitting roughly based on the calculated spectrum with corresponding characteristics.
255 The calculated spectra were shifted 72.2 eV.

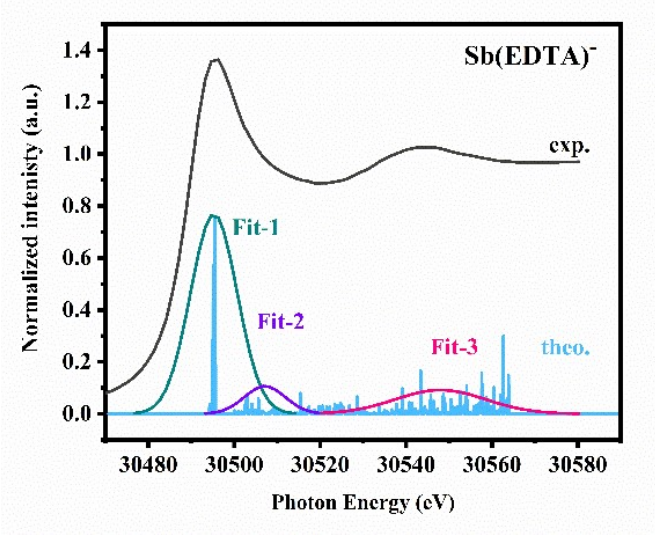


256

257 **Figure S9** Experimental and simulated Sb K-edge X-ray absorption spectrum of
258 $Sb(EDTA)^-$ complex. The subpeaks of experimental spectrum were result from peak
259 fitting roughly based on the calculated spectrum with corresponding characteristics.
260 The calculated spectra were shifted 70.7 eV.

261

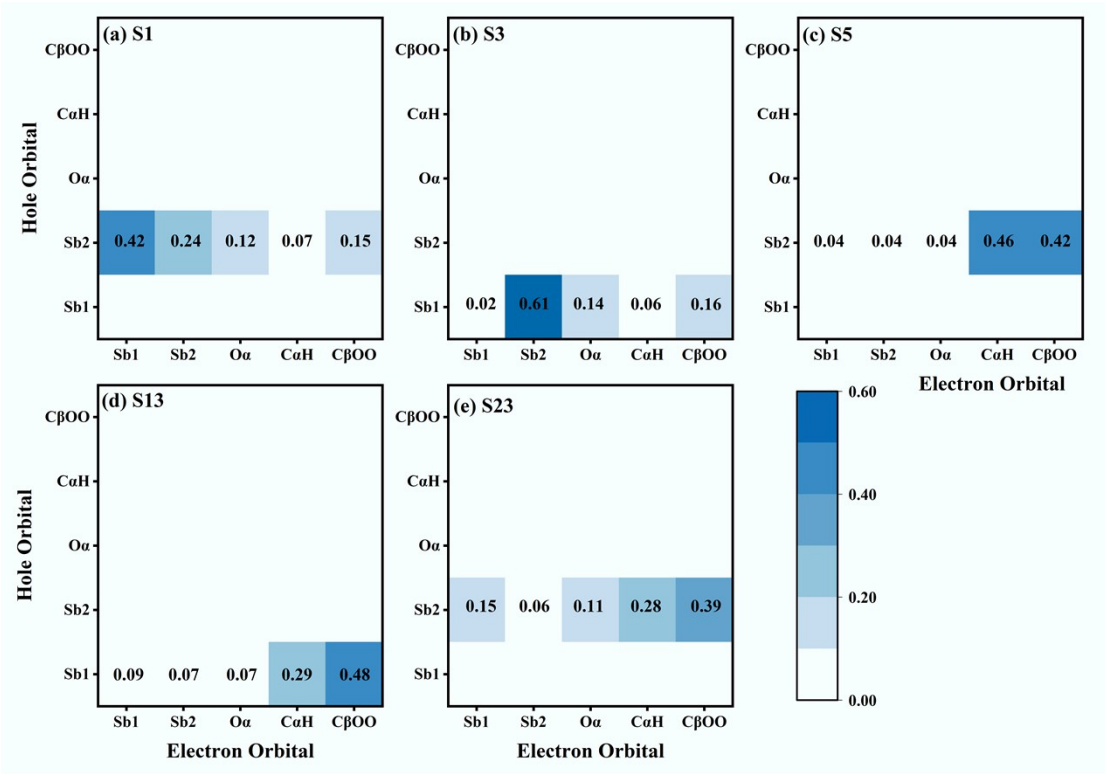


**Figure S10** Heat map for the transitions in $Sb_2(tar)_2^{2-}$ complex with IFCT analysis.

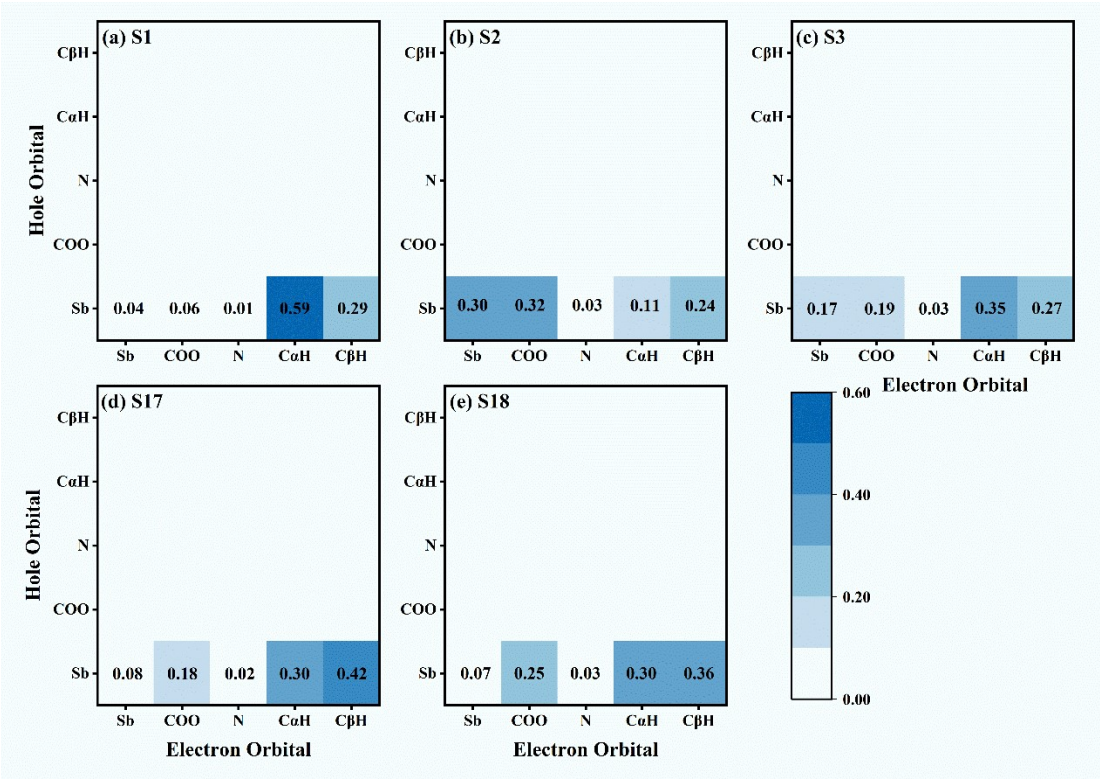


**Figure S11** Heat map for the transitions in Sb $(EDTA)^-$ complex with IFCT analysis.

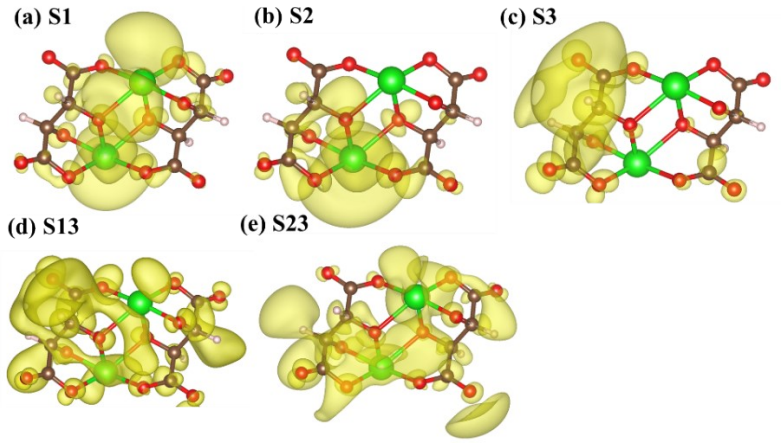


**Figure S12** Electron orbital for $Sb_2(tar)_2^{2-}$ complex.

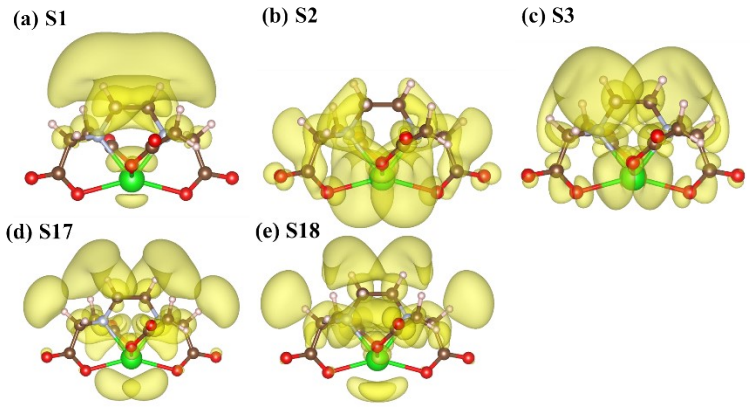


**Figure S13** Electron orbital for $Sb(EDTA)^-$ complex.

**Note S7** Definition of the parameter in NTO analysis and electron-hole analysis.

Process of single-electron excitation can be described as the electron transition from the hole orbital to the electron orbital. However, in most practical cases, the single MO pair representation is not suitable, excitations have to be represented as transition of multiple MO pairs with corresponding weighting coefficients. Therefore, the NTO or electron-hole analysis[5-7] were performed. The relevant concept based on this theory was detailed here.

(1) Density of hole and electron orbital ($\rho$)

The density of hole and electron orbitals rather than wavefunctions was used in form of

$\rho^{hole}(\mathbf{r})$ and $\rho^{ele}(\mathbf{r})$, where **r** is the position vector. The integral of the density to the whole space must be one.

$$\int \rho^{hole}(r)dr = 1$$

$$\int \rho^{ele}(r)dr = 1$$

(2) Centroid distance between hole and electron orbitals (*D*)

Centroid can be calculated to reveal most representative position of hole and electron distribution. The centroid (X, Y, Z) was the weighted average of the position of the orbitals where:

$$X_h = \int \rho^{hole}(x)xdx \; X_e = \int \rho^{ele}(x)xdx$$

$$Y_h = \int \rho^{hole}(y)ydy \; Y_e = \int \rho^{ele}(y)ydy$$

$$Z_h = \int \rho^{hole}(z)zdz \; Z_e = \int \rho^{ele}(z)zdz$$

Naturally, the centroid distance *D* was written as

$$D = \sqrt{(X_h - X_e)^2 + (Y_h - Y_e)^2 + (Z_h - Z_e)^2}$$

In this work, the centroid distance *D* was the charge transfer (CT) distance. The definition of the density and centroid distance *D* was identical for both of NTO analysis and electron-hole analysis.

(3) RMSD of hole and electron orbitals ($\sigma$)

The root mean square deviation (RMSD, $\sigma$) of the hole and electron orbitals can be used to characterize their extent of spatial distribution. The RMSD in different direction was defined as:

$$\sigma_{hole,x} = \sqrt{\int (x - X_h)^2 \rho^{hole}(x) dx} \quad \sigma_{ele,x} = \sqrt{\int (x - X_h)^2 \rho^{ele}(x) dx}$$

$$\sigma_{hole,y} = \sqrt{\int (y - Y_h)^2 \rho^{hole}(y) dy} \quad \sigma_{ele,y} = \sqrt{\int (y - Y_h)^2 \rho^{ele}(y) dy}$$

$$\sigma_{hole,z} = \sqrt{\int (z - Z_h)^2 \rho^{hole}(z) dz} \quad \sigma_{hole,z} = \sqrt{\int (z - Z_h)^2 \rho^{ele}(z) dz}$$

The overall RMSD of hole and electron orbital was defined as:

$$\sigma_{hole} = \sqrt{\sigma_{hole,x}^2 + \sigma_{hole,y}^2 + \sigma_{hole,z}^2}$$

$$\sigma_{ele} = \sqrt{\sigma_{ele,x}^2 + \sigma_{ele,y}^2 + \sigma_{ele,z}^2}$$

(4) Transition dipole moment ($\mu_{CT}$)

The transition dipole moment was defined as the vector of $\mu_{CT}$ in definition as:

$$\mu_{CT} = (-e(X_e - X_h),\ -e(Y_e - Y_h), -e(Z_e - Z_h))$$

(5) Spatial extension of hole and electron orbitals in CT direction ($H_{CT}$)

The hole and electron orbital extended to the whole space from the centroid with varied RMSD. The ***H*** vector (*H*x, *H*y, *H*z) measures average degree of spatial extension of hole and electron distribution in specific direction, where

$$H_x = \frac{\sigma_{hole,x} + \sigma_{ele,x}}{2} \quad H_y = \frac{\sigma_{hole,y} + \sigma_{ele,y}}{2} \quad H_z = \frac{\sigma_{hole,z} + \sigma_{ele,z}}{2}$$

The $\boldsymbol{H}_{CT}$ was the spatial extension of hole and electron orbitals in CT direction, therefore, it's defined as

$$H_{CT} = \frac{|H \cdot \mu_{CT}|}{|\mu_{CT}|}$$

(6) t index

The t index is used to measure separation degree of hole and electron in CT direction,

in definition of:

$$t = D - H_{CT}$$

(7) Overlap degree of hole and electron orbitals ($S^2$)

The overlap degree ($S^2$) was the integral of the product of density of hole and electron orbitals in any position with definition of:

$$S^2 = \int \rho^{hole}(r)\rho^{ele}(r)dr$$

This value was calculated via Becke's grid-based numerical integration approach rather than the analytical.

(8) $C_{ele}$

The density of electron orbital was smoothed with Gaussian-like function.

$$C_{ele}(r) = A_e exp( - \frac{(x - X_e)^2}{2\sigma_{e,x}^2} -- \frac{(y - Y_e)^2}{2\sigma_{e,y}^2} - \frac{(z - Z_e)^2}{2\sigma_{e,z}^2})$$

where $A_e$ was the normalized factor of the function.

**Table S15** Transition analysis for $Sb_2(tar)_2^{2-}$ complex

| No. | NTO analysis | | electron-hole analysis | | | | |
|---|---|---|---|---|---|---|---|
| | D (Å) | Overlap-$S^2$ | D (Å) | $\sigma_{hole}$ (Å) | $\sigma_{ele}$ (Å) | $H_{CT}$ (Å) | t (Å) |
| S1 | 2.41 | 0.289 | 2.39 | 0.00 | 2.99 | 0.88 | 1.51 |
| S3 | 3.64 | 0.008 | 3.67 | 0.05 | 2.35 | 0.69 | 2.98 |
| S5 | 2.89 | 0.024 | 2.86 | 0.00 | 3.52 | 1.05 | 1.81 |
| S13 | 1.93 | 0.028 | 1.93 | 0.05 | 3.68 | 1.21 | 0.72 |
| S23 | 1.75 | 0.020 | 1.73 | 0.00 | 3.95 | 0.99 | 0.74 |

**Table S16** Transition analysis for $Sb(EDTA)^-$ complex

| | NTO analysis | | electron-hole analysis | | | | |
|---|---|---|---|---|---|---|---|
| No. | D (Å) | Overlap-$S^2$ | D (Å) | $\sigma_{hole}$ (Å) | $\sigma_{ele}$ (Å) | $H_{CT}$ (Å) | t (Å) |
| S1 | 3.81 | 0.038 | 3.78 | 0.03 | 2.89 | 0.85 | 2.94 |
| S2 | 0.94 | 0.140 | 0.91 | 0.03 | 3.27 | 0.90 | 0.01 |
| S3 | 2.26 | 0.120 | 2.22 | 0.03 | 3.32 | 0.96 | 1.27 |
| S17 | 2.76 | 0.003 | 2.72 | 0.03 | 3.80 | 1.03 | 1.69 |
| S18 | 2.47 | 0.005 | 2.43 | 0.03 | 3.54 | 0.92 | 1.51 |

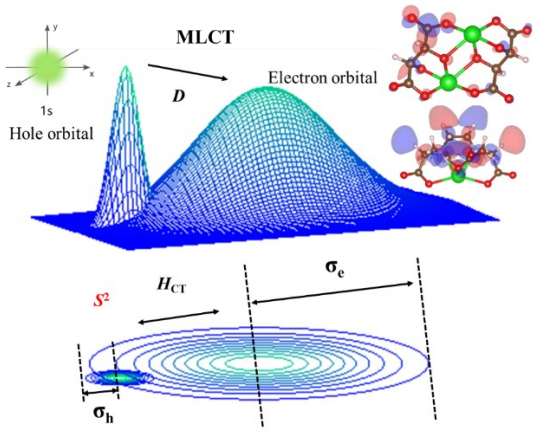


**Figure S14** Scheme of the charge transfer transition.

# References


1. W. Zhong, Z. Yin, L. Wang, L. Yan and C. Jing, *Chemosphere*, 2022, **301**, 134682.
2. G. Jansen and B. A. Hess, *Phys. Rev. A*, 1989, **39**, 6016-6017.
3. R. A. Kendall and H. A. Fruchtl, *Theor. Chem. Acc.*, 1997, **97**, 158-163.
4. S. Hirata and M. Head-Gordon, *Chem. Phys. Lett.*, 1999, **314**, 291-299.
5. Z. Y. Liu, T. Lu and Q. X. Chen, *Carbon*, 2020, **165**, 461-467.
6. X. Tang, L. S. Cui, H. C. Li, A. J. Gillett, F. Auras, Y. K. Qu, C. Zhong, S. T. E. Jones, Z. Q. Jiang, R. H. Friend and L. S. Liao, *Nat. Mater.*, 2020, **19**, 1332-1338.
7. T. Lu and F. W. Chen, *J. Comput. Chem.*, 2012, **33**, 580-592.